GPR18 is required for a normal CD8αα intestinal intraepithelial lymphocyte compartment

Xiaoming Wang,[1,2*] Hayakazu Sumida,[1,2] and Jason G. Cyster[1,2]

[1]Howard Hughes Medical Institute and [2]Department of Microbiology and Immunology, University of California, San Francisco, San Francisco, CA 94143

Intraepithelial lymphocytes (IELs) play an important role in maintaining the physiology of the small intestine. The majority of mouse IELs express CD8αα and are either γδ or αβ T cells. Although the development and homing of CD8αα IELs have been studied in some detail, the factors controlling their homeostasis and positioning are incompletely understood. Here we demonstrate that G protein–coupled receptor 18 (GPR18) is abundantly expressed in CD8αα IELs and that mice lacking this orphan receptor have reduced numbers of γδT IELs. Mixed bone marrow chimera experiments reveal a markedly reduced contribution of GPR18-deficient cells to the CD8αα IEL compartment and a reduction in the CD8αβ T cell subset. These defects could be rescued by transduction with a GPR18-expressing retrovirus. The GPR18-deficient γδT IELs that remained in mixed chimeras had elevated Thy1, and there were less granzyme B$^+$ and Vγ7$^+$ cells, indicating a greater reduction in effector-type cells. Flow cytometric analysis indicated GPR18 deficiency more strongly affected the CD8αα cells in the intraepithelial compared with the adjacent lamina propria compartment. These findings establish a requirement for GPR18 in CD8αα and CD8αβ IELs, and we suggest the receptor has a role in augmenting the accumulation of CD8 T cells in the intraepithelial versus lamina propria compartment.

CORRESPONDENCE
Jason G. Cyster:
Jason.Cyster@ucsf.edu

Abbreviations used: AHR, aryl hydrocarbon receptor; IEL, intraepithelial lymphocyte; LPL, lamina propria lymphocyte; mLN, mesenteric LN; QPCR, quantitative PCR.

Distributed along the length of the small intestine at a density of ∼1 per 10 epithelial cells, intraepithelial lymphocytes (IELs) constitute a large population of barrier immune cells (Hayday et al., 2001; Abadie et al., 2012). In mice the majority of IELs express the CD8αα homodimer, and 40–60% bear a γδTCR (Hayday et al., 2001; Cheroutre et al., 2011). γδT IELs are predominantly Vγ7$^+$ (nomenclature of Heilig and Tonegawa [1986]), and they contribute to maintaining intestinal barrier function in the healthy state and during mucosal infections (Cheroutre et al., 2011; Abadie et al., 2012). In humans, IEL numbers increase in several conditions, including inflammatory bowel disease, and epithelial γδT lymphocytosis is a marker of celiac disease progression (Cheroutre et al., 2011; Abadie et al., 2012). γδT IELs develop from double-negative thymic precursors and undergo further maturation in the periphery before taking on a mature Thy1^{lo}, granzyme B^{hi} IEL phenotype (Johansson-Lindbom and Agace, 2007; Ma et al., 2009; Guy-Grand et al., 2013). CD8αα αβT IELs develop from a unique self-reactive subset of double-positive thymocytes (Lambolez et al., 2007). The less abundant CD8αβ TCRαβ and minor CD4 TCRαβ IEL subsets represent mucosa-homing effector lymphocytes and are closely related to the main lamina propria T cell populations (Arstila et al., 2000; Cheroutre et al., 2011). CD8αα γδT and αβT IELs, but not CD8αβ IELs, are dependent on IL15 and the aryl hydrocarbon receptor (AHR), and epithelial cells are a necessary source of the trans-presenting IL15Rα chain (Abadie et al., 2012).

The intestinal epithelium is separated from the lamina propria by a basement membrane (Edelblum et al., 2012). As well as having a rich supply of blood and lymphatic vessels, the lamina propria contains T cells, dendritic cells, and plasma cells. The T cells are predominantly

*X. Wang's present address is Dept. of Immunology, Nanjing Medical University, Nanjing 210029, China.

The Rockefeller University Press $30.00
J. Exp. Med. 2014 Vol. 211 No. 12 2351–2359
www.jem.org/cgi/doi/10.1084/jem.20140646

CD4 αβT cells, and there are very few cells with an IEL phenotype in the lamina propria (Cheroutre et al., 2011). The chemokine CCL25 (TECK) and its receptor CCR9 play a crucial role in T cell and plasma cell homing to the small intestinal intraepithelial and lamina propria compartments (Kunkel et al., 2003; Pabst et al., 2004; Stenstad et al., 2007; Wurbel et al., 2007). CCL25 is expressed by small intestinal epithelial cells, with expression being highest in the duodenum and decreasing incrementally in the jejunum and ileum (Stenstad et al., 2007). Mice lacking CCL25 or CCR9 exhibit 3- to 10-fold reductions in γδT CD8αα IELs (Wurbel et al., 2001, 2007; Uehara et al., 2002), and homing of mucosally activated effector CD8 T cells to the intestine is compromised (Stenstad et al., 2007; Wurbel et al., 2007). CCL25 and CCR9 deficiency was also shown to cause a reduction in CD8 but not CD4 T cell frequencies in the lamina propria (Wurbel et al., 2007). CD8αα αβT IEL numbers were not reduced in CCR9- or CCL25-deficient mice despite similar CCR9 expression on CD8αα γδT and αβT IELs (Wurbel et al., 2001, 2007; Uehara et al., 2002). CD8αβ and CD4 IEL numbers were also not reduced. The migration dynamics of IELs in the steady-state has recently been examined by two-photon microscopy (Chennupati et al., 2010; Edelblum et al., 2012). One study suggested the cells were mostly immobile (Chennupati et al., 2010), whereas a second provided evidence that they moved dynamically within and between intraepithelial niches (Edelblum et al., 2012). Despite these advances, the mechanisms controlling the homeostasis and positioning of the different intestinal T cell subsets remain incompletely understood.

Here we identify a role for a novel G protein–coupled receptor, GPR18, in promoting the maintenance of small intestinal CD8αα γδT, αβT, and CD8αβ IELs, and we provide evidence that this receptor favors positioning of CD8αα γδT cells in the intraepithelial versus lamina propria compartment.

RESULTS AND DISCUSSION

GPR18 is highly expressed in lymphoid tissues and is widely expressed in immune cells, being abundant in splenic T and B cells (Fig. 1 A). Public domain gene expression data indicated two- to threefold higher expression of GPR18 in intestinal IELs compared with splenic T cells (http://www.immgen.org; http://refdic.rcai.riken.jp), and this was confirmed in quantitative PCR (QPCR) analysis of sorted cells, with expression being highest on CD8αα γδT IELs and CD8αα αβT IELs, followed by CD8αβ αβT IELs (Fig. 1 A). GPR18 transcript abundance in intestinal CD4 αβT cells, which are rare within IEL preparations (∼5%) and are much more abundant in the lamina propria (∼30%), was similar to the expression level in splenic lymphocytes (Fig. 1 A). To examine the role of GPR18 in lymphocytes, we generated GPR18-deficient mice by gene targeting. GPR18-deficient mice had normal numbers of splenic and LN αβ and γδT cells and B cells, and lymphocyte development in thymus and BM appeared normal (not depicted). Analysis of IELs showed there were similar numbers of total cells in matched adult (2–3 mo old) control and *Gpr18*$^{-/-}$ mice (Fig. 1 B). However, when the IEL subsets were examined, *Gpr18*$^{-/-}$ mice exhibited a selective deficiency in CD8αα γδT IELs (Fig. 1 C). The properties of the IEL compartment are known to change with age (Laky et al., 1997; Cheroutre et al., 2011), and analysis of a group of aged (∼7 mo old) *Gpr18*$^{-/-}$ and littermate control mice showed that there was now a significant reduction in total IEL numbers (Fig. 1 D). The CD8αα γδT IEL compartment continued to be the most affected (approximately fourfold reduced, $P < 0.01$), but CD8αα and CD8αβ αβT cell numbers were also reduced (approximately twofold, $P < 0.05$, $n = 6$; not depicted).

GPR18 has been suggested to promote cell chemotaxis in a Gαi protein–coupled manner to the endocannabinoid *N*-arachidonoyl-glycine (Kohno et al., 2006; McHugh et al., 2012). However, when WEHI231 B cells transduced with GPR18 were tested for responses to this ligand, no migration was observed, whereas the same cells transduced with several other receptors, including the endocannabinoid receptor CB2, the oxysterol receptor EBI2, the sphingosine-1-phosphate receptor S1PR1, and the chemokine receptor CXCR5, showed robust migratory responses to the appropriate ligands (Fig. 1 E and not depicted). The inability of GPR18 to respond to *N*-arachidonoyl-glycine was also noted in a study using β-arrestin recruitment to assess GPCR activation (Yin et al., 2009). Although we could not confirm *N*-arachidonoyl-glycine as a ligand for GPR18, we did observe that transduction of WEHI231 cells with GPR18 led to an approximately fivefold reduction in the CXCR4-mediated chemotactic response to CXCL12 (Fig. 1 E). This type of inhibitory effect is seen after transduction of WEHI231 cells with a range of established Gαi-coupled receptors, including CB2, EBI2, and S1PR1 (Fig. 1 E and not depicted), but does not occur when the cells are transduced with GPCRs that are established not to be Gαi coupled, including the thromboxane A2 receptor (TBXAR2) and S1PR2 (Fig. 1 E and not depicted). Based on these data, we suggest that GPR18 is effective in competing for Gαi binding and that it may therefore be able to couple to this G protein and have a pro-migratory role.

Analysis of duodenum sections for the distribution of γδT IELs showed that although reduced in frequency in the GPR18-deficient tissue, the CD8α γδT double-positive cells were distributed similarly in both types of mice, with most being in an intraepithelial location (Fig. 1 F). The migration dynamics of γδT IELs has recently been studied using real-time intravital imaging with discrepant findings regarding whether the cells are largely immobile (Chennupati et al., 2010), like dendritic epidermal T cells in the skin (Gray et al., 2011; Sumaria et al., 2011), or whether they are motile (Edelblum et al., 2012). To further examine whether IELs are motile and test whether GPR18 deficiency affected their movement dynamics, we developed a procedure to intravitally label CD8α$^+$ IELs. Systemic injection of anti–CD8α-PE 5 h before analysis led to uniform labeling of CD8α$^+$ cells in the epithelial and lamina propria compartments (Fig. 1 G). Using two-photon microscopy to image CD8α$^+$ IELs from the luminal side of duodenal villi, we observed WT cells moving

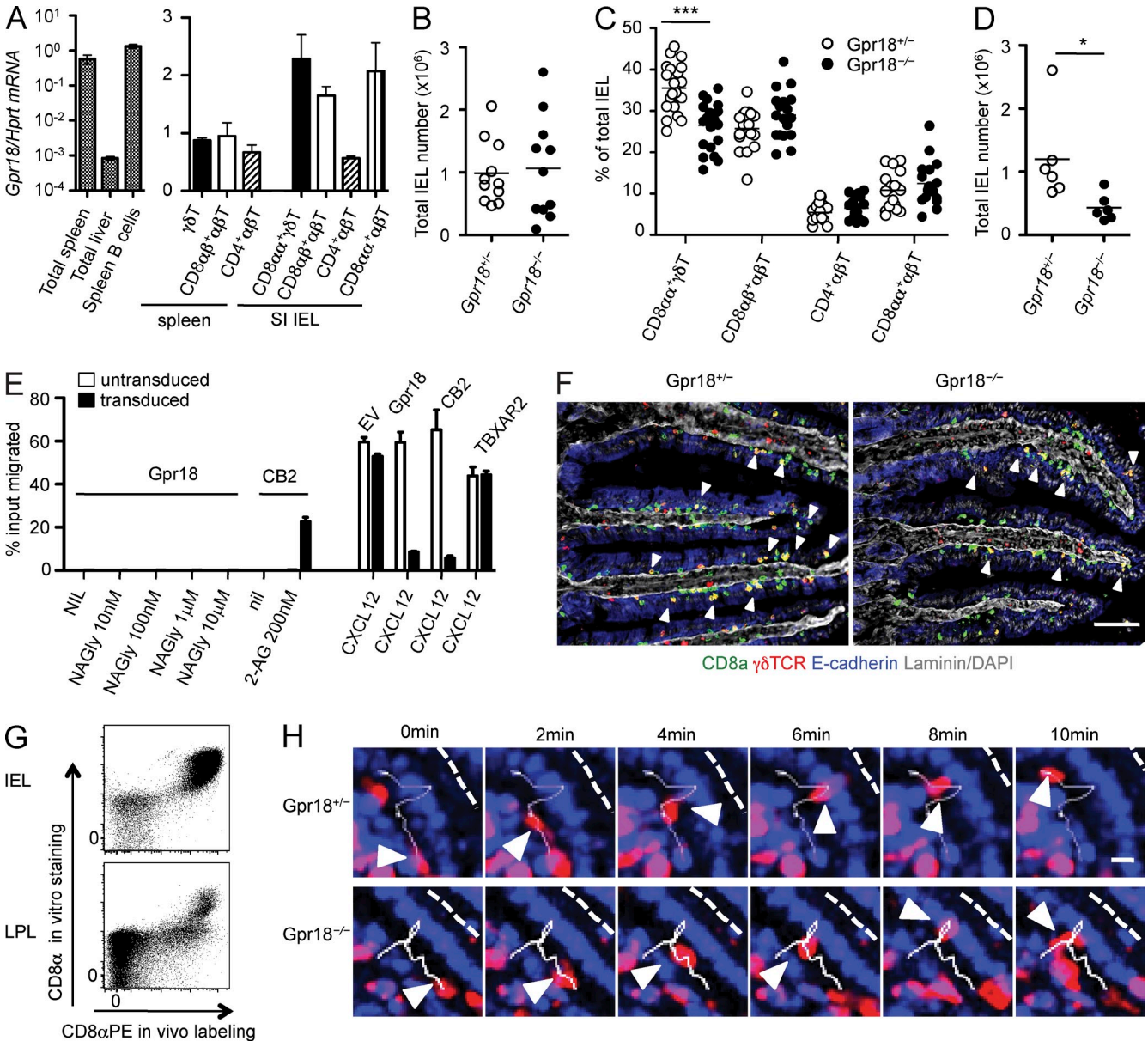

Figure 1. Reduction of CD8αα γδT IELs in GPR18-deficient mice. (A) QPCR analysis of *Gpr18* mRNA transcript abundance in spleen, liver, and sorted spleen cells and small intestine (SI) IELs as indicated, presented relative to *Hprt*. (B) Total SI IEL numbers of $Gpr18^{+/-}$ and $Gpr18^{-/-}$ mice. (C) Percentage of indicated subsets among total IELs from $Gpr18^{+/-}$ and $Gpr18^{-/-}$ mice. CD8αα cells were gated as $CD8\alpha^{+}CD8\beta^{-}$. Mice in B and C were 2–3 mo old. ***, $P \leq 0.001$ (Student's *t* test). (D) Total SI IEL numbers in aged (~7 mo old) $Gpr18^{+/-}$ and $Gpr18^{-/-}$ mice. *, $P < 0.05$ (Student's *t* test). (E) Transwell migration assay of WEHI231 cells transduced with the retroviral vectors as labeled, in response to the indicated ligands. CXCL12 concentration was 100 ng/ml. (A and E) Data are shown as mean ± SD. EV, empty vector; NAGly, *N*-arachidonoyl-glycine; 2-AG, 2-arachidonyl-glycerol. (F) Immunofluorescent staining of IELs in duodenum from $Gpr18^{+/-}$ and $Gpr18^{-/-}$ mice. Arrowheads highlight CD8α and γδTCR double-positive (yellow) cells. (G) Flow cytometric analysis of IELs and LPLs from a mouse injected 5 h earlier with anti-CD8α-PE. (H) Time-lapse images of duodenum of $Gpr18^{+/-}$ and $Gpr18^{-/-}$ mice. CD8α-PE (red) and nuclei (DAPI, blue) are shown. Dashed line indicates the interface between the epithelium and the intestinal lumen. Arrowheads point to the location of one tracked $CD8\alpha^{+}$ cell at each time point, and lines indicate tracked paths. Bars: (F) 100 µm; (H) 10 µm. In B–D each symbol represents an individual mouse, and the horizontal line indicates the mean. Data in A, E, F, and H are representative of three experiments.

up and down the lateral intercellular junctions of epithelial cells, migrating between epithelial cells via the subepithelial space, and occasionally accessing the lamina propria (Fig. 1 H and Video 1). These behaviors for total $CD8\alpha^{+}$ IELs are similar to the findings of Edelblum et al. (2012) for γδT IELs using TcrdEGFP reporter mice, supporting the conclusion that IELs are motile and suggesting that the major IEL populations (CD8αα γδT and αβT) have similar movement dynamics. Analysis of GPR18-deficient mice using the same intravital CD8α-labeling procedure revealed that, at the level

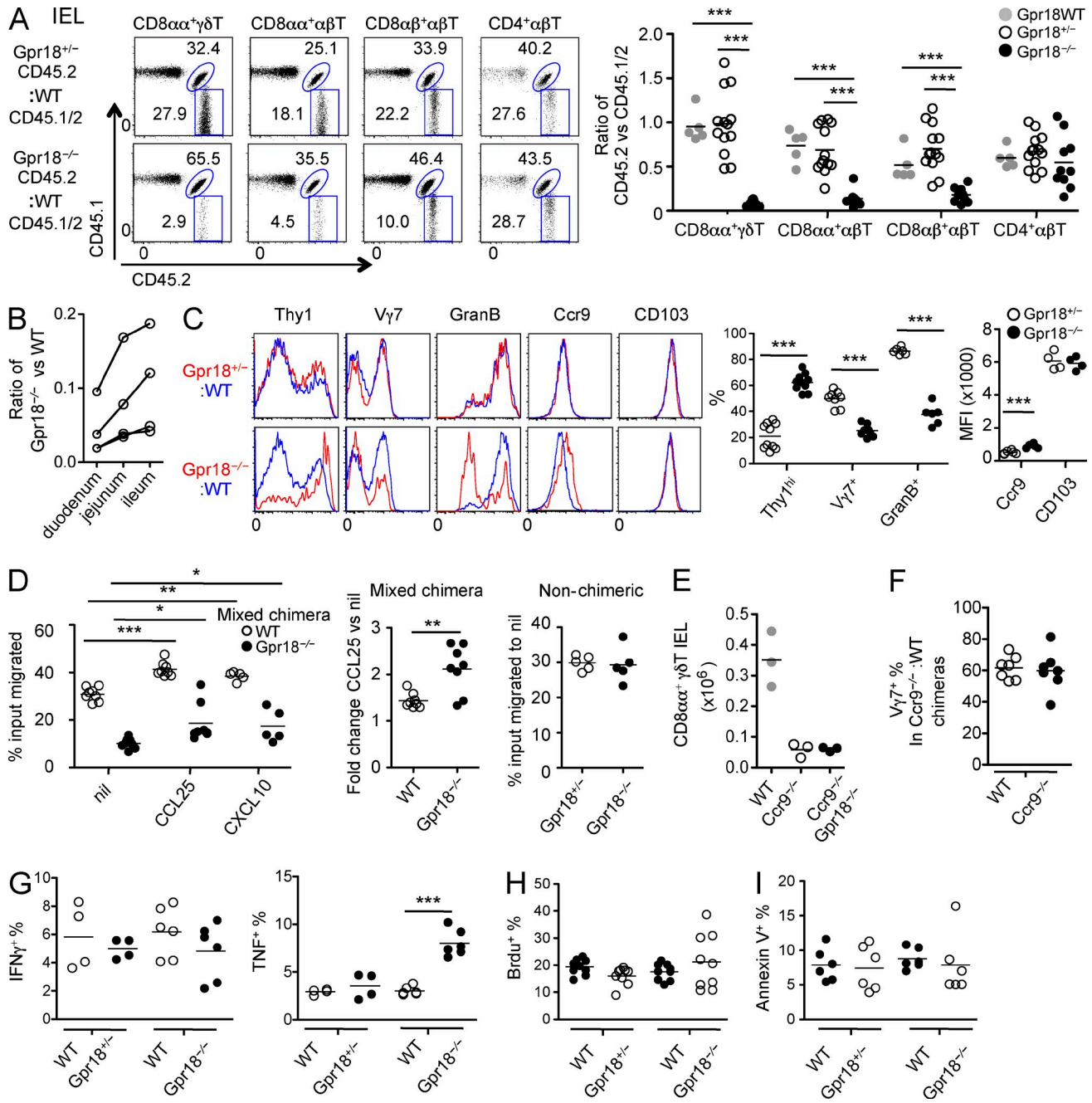

Figure 2. Marked reduction of CD8α IELs in GPR18-deficient mixed BM chimeras. (A) B6-CD45.1+ mice were reconstituted with 50% CD45.1/2+ WT and 50% CD45.2+ WT, *Gpr18*$^{+/-}$, or *Gpr18*$^{-/-}$ BM 2–3 mo before analysis. IELs were stained for the subsets as indicated. Numbers indicate percentage of cells in each gate. CD45.1+CD45.2− cells are radiation-resistant host cells. Ratios of WT, *Gpr18*$^{+/-}$, or *Gpr18*$^{-/-}$ CD45.2+ cells versus WT CD45.1/2+ cells were plotted. (B) Ratios of *Gpr18*$^{-/-}$ versus WT CD8αα γδT IELs in different small intestine segments of mixed chimeras. The ratios were connected for each mouse. (C) Flow cytometry analysis of the indicated markers in the CD8αα γδT IELs from mixed chimeras. Graphs on the right show summary of data from several experiments, where % indicates fraction of cells positive for the marker and MFI indicates mean fluorescence index. Data are representative of more than five experiments in A and three experiments in B and C. (D) Transwell migration assay of CD8αα γδT IELs from mixed chimeras (left and middle) or nonchimeric mice (right) of the type indicated in response to medium alone (nil), 5 µg/ml CCL25, or 1 µg/ml CXCL10, shown as percentage of input cells that migrated. Graph on right shows the fold change in γδT IEL migration in response to CCL25 versus no chemokine. Data are representative of four experiments. (E) Number of CD8αα γδT IELs in WT, *Ccr9*$^{-/-}$, and *Ccr9*$^{-/-}$ *Gpr18*$^{-/-}$ mice. (F) Frequency of Vγ7+ cells among CD8αα γδT IELs of WT and *Ccr9*$^{-/-}$ origin in WT:*Ccr9*$^{-/-}$ mixed chimeras. (G) Intracellular staining of stimulated CD8αα γδT IELs from mixed chimeras for IFN-γ and TNF, shown as frequency of positive cells. (H) Frequency of CD8αα γδT IELs in mixed chimeras that were positive for BrdU staining after 1 wk of in vivo labeling. (I) Frequency of CD8αα γδT IELs in mixed chimeras that were Annexin V+ by flow cytometric analysis. *, $P < 0.05$; **, $P < 0.01$; ***, $P \leq 0.001$ (Student's *t* test). In D, the migration of *Gpr18*$^{-/-}$ cells was significantly reduced compared with WT ($P < 0.001$). In A and C–I each symbol represents an individual mouse, and the horizontal lines indicate the mean.

that could be resolved with our current imaging platform, their CD8α$^+$ IEL migration dynamics were indistinguishable from those of the controls (Fig. 1 H and Video 2).

To further probe the stage at which GPR18 was influencing the accumulation of CD8αα γδT IELs, and to test whether the requirement was cell intrinsic, we generated mixed BM chimeras. This analysis revealed that even under conditions of competition there was no effect of GPR18 deficiency on CD4 or CD8 T cell numbers in the spleen or LNs (not depicted). However, within the IEL compartment there was a marked (~10-fold) defect in CD8αα γδT cells and there was now also a reduction in CD8αα αβT cells (~5-fold) and CD8αβ αβT cells (~3-fold), whereas CD4 αβT cells were unaffected (Fig. 2 A). A comparison of the ratio of GPR18-deficient and WT γδT IELs along the length of the small intestine revealed a graded effect with the strongest defect being in the duodenum (Fig. 2 B). The basis for the greater impact of GPR18 deficiency under competitive compared with noncompetitive conditions is not known, but might indicate a reduced ability compared with WT cells to access or use a maturation signal or trophic factor that is in limited supply.

Surface phenotyping revealed that the *Gpr18*$^{-/-}$ γδT IELs in the mixed BM chimeras were enriched for Thy1^{hi} cells and were depleted for the major γδTCR typical of intestinal IELs, Vγ7 (Fig. 2 C). The *Gpr18*$^{-/-}$ IELs were also depleted for granzyme B–high cells (Fig. 2 C). The high Thy1 and low granzyme B expression is consistent with a less mature effector state (Ma et al., 2009; Cheroutre et al., 2011). CD103 (αE integrin) expression was comparable on the *Gpr18*$^{-/-}$ and control cells, whereas CCR9 and CXCR3 surface levels were slightly elevated (Fig. 2 C and not depicted). Contrary to this elevated CCR9 and CXCR3 expression, GPR18-deficient γδT IELs in mixed BM chimeras showed reduced migration to the CCR9 ligand, CCL25, and the CXCR3 ligand, CXCL10 (Fig. 2 D). However, they also had a significantly reduced baseline migration in the absence of chemokine (Fig. 2 D). When the fold change in migration compared with "nil" was determined, there was an increase in the relative CCL25 response of the *Gpr18*$^{-/-}$ cells (Fig. 2 D). The alterations in CD8αα γδT cell surface phenotype and migration behavior observed for *Gpr18*$^{-/-}$ cells from mixed BM chimeras (Fig. 2, C and D) were not seen for CD8αα γδT cells from *Gpr18*$^{-/-}$ mice (Fig. 2 D and not depicted). This may indicate that these phenotypes are secondary consequences of a role played by GPR18 in helping cells to compete for a maturation signal.

CCR9-deficient mice suffer a deficiency in CD8αα γδT IEL numbers (Wurbel et al., 2001, 2007; Uehara et al., 2002) that is more severe than observed in GPR18-deficient mice (Fig. 2 E and Fig. 1 C). Analysis of CCR9 GPR18 double-deficient mice showed a similar magnitude of CD8αα γδT IEL deficiency to that observed in *Ccr9*$^{-/-}$ mice (Fig. 2 E). These data suggest the function of CCR9 is dominant over the role of GPR18 in establishing an IEL compartment of normal size. However, in contrast to *Gpr18*$^{-/-}$ γδT IELs in

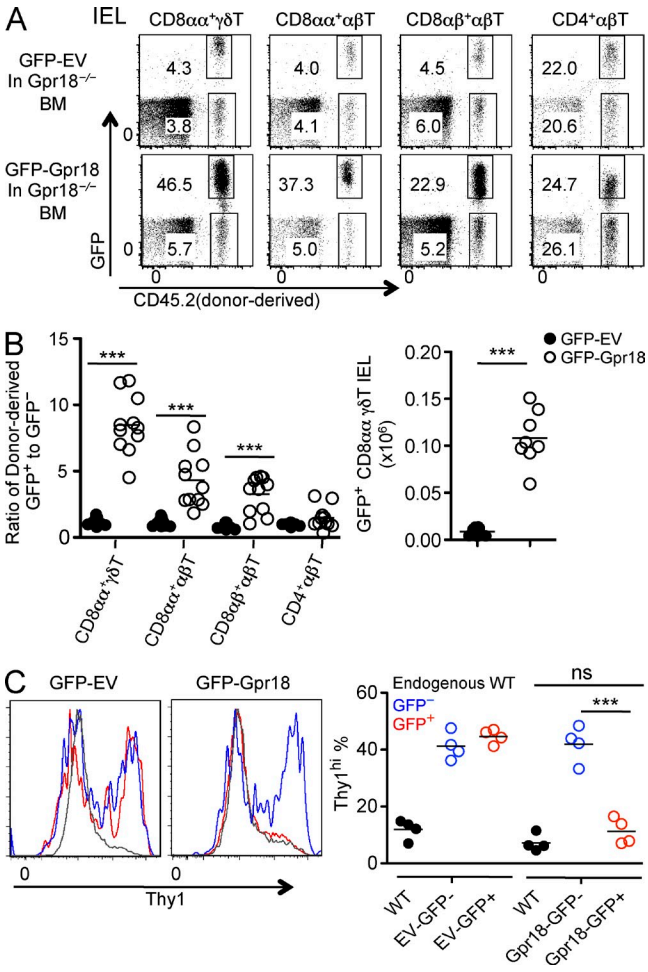

Figure 3. GPR18 expression rescues the IEL defect in *Gpr18*$^{-/-}$ mice. (A) CD45.2$^+$ *Gpr18*$^{-/-}$ BM transduced with empty vector (GFP-EV) or GFP-Gpr18 retrovirus was used to reconstitute CD45.1$^+$ recipients. IELs were stained for the subsets as indicated. Numbers indicate percentage of cells in each gate. (B) Summary data of the type in A, shown as the ratio of donor-derived GFP$^+$ to GFP$^-$ cells of the indicated types (left) or as number of GFP$^+$ CD8αα γδT IELs (right). (C) Flow cytometry of Thy1 expression in the CD8αα γδT IELs from BM chimeras, color coded as on the right. Graph shows summary data for the frequency of Thy1^{hi} cells in the same gated CD8αα γδT IEL populations (GFP$^+$ and GFP$^-$ *Gpr18*$^{-/-}$ CD45.2$^+$ and endogenous radio-resistant WT CD45.1$^+$ cells). Each symbol in B and C represents an individual mouse, and the small horizontal lines indicate the mean. ***, P ≤ 0.001 (Student's *t* test). Data are representative of three experiments.

mixed BM chimeras (Fig. 2 C), *Ccr9*$^{-/-}$ γδT IELs in mixed BM chimeras contained normal Vγ7$^+$ cell frequencies (Fig. 2 F). These findings indicate that GPR18 has a function distinct from or in addition to any role it might have in supporting CCR9 function.

Analysis of cytokine production after in vitro activation of cells from mixed BM chimeras revealed similar IFN-γ expression by *Gpr18*$^{-/-}$ and internal control cells but elevated TNF production by the *Gpr18*$^{-/-}$ cells (Fig. 2 G). The TNF expression level was similar to that observed in Thy1^{hi} WT cells (not depicted), suggesting that it was secondary to the

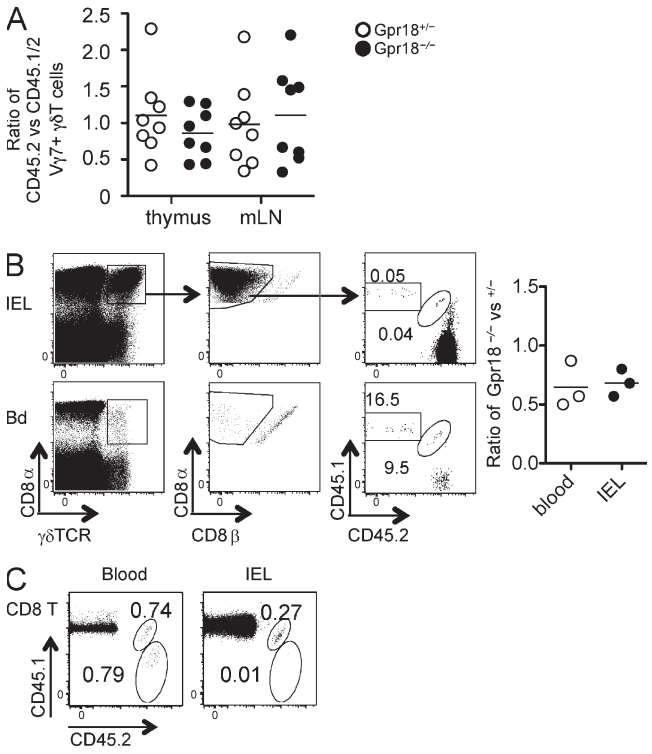

Figure 4. Normal IEL precursor development and intestinal homing in the absence of GPR18. (A) Mixed BM chimeras of the type in Fig. 2 were analyzed for Vγ7$^+$ γδT cells in thymus and mLN. Thymic cells were gated as CD8$^-$CD4$^-$TCRβ$^-$ γδTCR$^+$Vγ7$^+$ and mLN cells as TCRβ$^-$ γδTCR$^+$Vγ7$^+$, and the data are plotted as the ratio of gated cells that were CD45.2$^+$ (*Gpr18*$^{+/-}$ or *Gpr18*$^{-/-}$) versus CD45.1/2$^+$ (WT). (B) IELs from *Gpr18*$^{+/-}$ (CD45.1$^+$) and *Gpr18*$^{-/-}$ (CD45.1/2$^+$) mice were co-transferred into *Ccr9*$^{-/-}$ recipients. 20 h later, the distribution of transferred CD8αα γδT IELs in blood (Bd) and intestine IELs was analyzed by flow cytometry. The plot on the right shows the ratio of *Gpr18*$^{-/-}$ versus *Gpr18*$^{+/-}$ donor cell frequencies in blood and IELs, summarized from three experiments. (C) LN T cells from WT (CD45.1/2$^+$) and *Ccr9*$^{-/-}$ (CD45.2$^+$) mice were stimulated with CD3/CD28 plus retinoic acid and co-transferred into CD45.1$^+$ WT hosts. 20 h later, the distribution of transferred CD8 T cells in blood and IELs was analyzed by flow cytometry. Data are representative of three or more experiments in A and B and of two mice in C. In A and B each symbol represents an individual mouse, and the horizontal lines indicate the mean.

effect of GPR18 deficiency on cell maturation state in competitive chimeras. To examine the IEL turnover rate, mixed BM chimeras were maintained on drinking water containing BrdU for 1 wk and then examined by flow cytometry. Similar fractions of control and *Gpr18*$^{-/-}$ cells were BrdU labeled (Fig. 2 H), suggesting that the reduced *Gpr18*$^{-/-}$ cell number was not a consequence of a markedly accelerated loss of IELs. Consistent with this conclusion, the fraction of apoptotic γδT IELs detected by annexin V staining was similar for the mutant and WT cells (Fig. 2 I).

To confirm that the deficiency in IELs was solely caused by a loss of GPR18 and not caused by altered expression of a linked gene or other off-target effects, GPR18 expression was rescued in *Gpr18*$^{-/-}$ BM by retroviral transduction. Analysis of spleen cells from mice reconstituted with GPR18-encoding versus control retrovirus–transduced BM showed that reporter-positive cells were present at similar frequencies in both groups, confirming that GPR18 does not influence the development of recirculating T cell populations (not depicted). However, within the intestine, each of the IEL subsets that were deficient in the absence of GPR18 was markedly rescued by GPR18 transduction (Fig. 3 A). This was evident both as a higher frequency of transduced (reporter positive) cells and an increase in their number to within twofold of the normal range (Fig. 3 B and Fig. 1, B and C). Moreover, the rescued CD8αα γδT cells down-regulated Thy1 to a similar extent as control cells (Fig. 3 C).

Vγ7$^+$ IELs are generated in the thymus and may undergo a final maturation process in mesenteric LNs (mLNs; Guy-Grand et al., 2013). Production of Vγ7$^+$ γδT cells in the thymus of mixed BM chimeras was not affected by GPR18 deficiency (Fig. 4 A and not depicted). The cells were also present in frequencies comparable with those of *Gpr18*$^{+/-}$ controls in the mLNs (Fig. 4 A and not depicted). To test whether homing of IELs from blood to intestine might require GPR18, a mixture of total IELs from GPR18-deficient (CD45.1/2) and WT (CD45.1) donors were transferred to γδT IEL-deficient (*Ccr9*$^{-/-}$ CD45.2) recipients. Although CD8αα IELs are nonrecirculatory and home only inefficiently back to the small intestine after i.v. transfer (Hayday et al., 2001; Chennupati et al., 2010; Cheroutre et al., 2011), analysis at 1 d showed that *Gpr18*$^{-/-}$ cells were present among the transferred cells within the IEL compartment at a similar frequency to their representation in blood (Fig. 4 B). These data disfavor a role for GPR18 in promoting CD8αα IEL recruitment from blood into tissue. Given that GPR18 is thought to most likely respond to a small molecule ligand (Inoue et al., 2012), these findings are not unexpected as the step of lymphocyte recruitment from blood into tissue usually involves a protein (chemokine) ligand that can be displayed on the endothelium (Islam and Luster, 2012). CCR9 and CCL25 are established to play an important role in this recruitment step for CD8 T cells and plasma cells (Kunkel et al., 2003; Pabst et al., 2004; Stenstad et al., 2007; Wurbel et al., 2007), a requirement we could confirm for CD8 T cells that had been activated under CCR9-inducing conditions (Fig. 4 C).

CD8αα IELs are considered to be restricted to the intraepithelial compartment, and consistent with this view, the cells make up only a very minor component of standard lamina propria lymphocyte (LPL) preparations (Fig. 5 A; Cheroutre et al., 2011), and it has so far not been possible to determine their distribution in the lamina propria by immunofluorescence analysis. However, because our intravital imaging and that of Edelblum et al. (2012) suggested that CD8α$^+$ IELs occasionally access the lamina propria (Videos 1 and 2), we asked whether GPR18 differentially affected the frequency of CD8αα γδT cells in these compartments. Analysis of IEL and LPL preparations from mixed BM chimeras revealed that the fraction of CD8αα γδT and αβT IELs was more strongly reduced in the IEL compartment than within the

LPL compartment (Fig. 5 B). Reciprocally, in mice reconstituted with GPR18-tranduced *Gpr18*$^{-/-}$ BM, the reporter-positive CD8αα γδT cells were enriched in the IEL compared with the LPL compartment (Fig. 5 C). These observations suggest that GPR18 augments access of CD8αα γδT cells to, or retention within, the IEL compartment.

In summary, we establish that the orphan receptor, GPR18, is required for the normal homeostasis of CD8αα γδT and αβT IELs and CD8αβ IELs. Our intravital imaging helps resolve a discrepancy between two recent studies (Chennupati et al., 2010; Edelblum et al., 2012) by providing additional evidence that IELs are motile and that they do not remain fixed between one set of epithelial cells but travel between intraepithelial niches through a path that sometimes takes them into the lamina propria. Studies on other cell types, such as germinal center and marginal zone B cells (Allen et al., 2004; Arnon et al., 2011), indicate that for cells to move repeatedly between adjacent compartments, they need to respond to at least two GPCR ligands that are distributed unequally between the compartments. The only directional cue previously established to promote IEL positioning in the small intestine is CCL25 and its receptor CCR9, and at steady-state these studies only found effects on γδT IELs (Abadie et al., 2012; Islam and Luster, 2012). Based on our findings here, we suggest that GPR18 may respond to a ligand that is distributed in areas overlapping with but not identical to the distribution of CCL25 and that the receptor helps achieve fine control of IEL distribution within the small intestine. We suggest that by affecting the efficiency of access to currently imprecisely defined intestinal niches, GPR18 influences exposure of IELs to factors necessary for their maturation or trophic support and that the reduced ability to access these factors most strongly affects their numbers under conditions of competition. Strong competitive effects on cell numbers have been observed in other instances where trophic support is limited (e.g., Lesley et al., 2004; Thien et al., 2004). The altered maturation state may in turn be responsible for the reduced in vitro motility of the cells, an alteration which might amplify effects of GPR18 deficiency on cell positioning and homeostasis. It is notable that mice lacking IL15Rα or AHR have decreased CD8αα IELs but retain normal numbers of CD8αβ IELs (Lodolce et al., 1998; Ma et al., 2009; Li et al., 2011). The reduced competitiveness of GPR18-deficient CD8αβ as well as CD8αα IELs indicates GPR18 may be required for accessing factors in addition to or other than IL15 or AHR ligands or that it is instead required for retention of IELs in the intestine. We do not exclude the possibility that GPR18 transmits signals that have their own trophic or maturational influence on IELs. It will be important in future studies to define the nature of the GPR18 ligand and to study whether GPR18 and GPR18 ligand abundance are altered in disease states where γδT IEL numbers and distribution are affected, such as in inflammatory bowel disease and celiac disease (Cheroutre et al., 2011; Abadie et al., 2012).

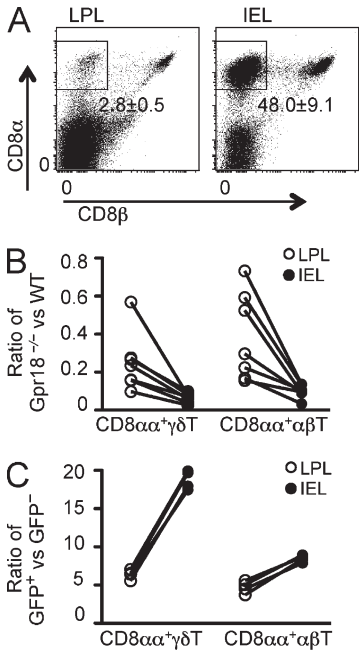

Figure 5. Differential GPR18-deficient cell distribution in IEL and LPL compartments. (A) CD8αα cell frequency in IELs and LPLs by flow cytometry analysis. Percentages are shown as mean ± SD. (B) *Gpr18*$^{-/-}$ mixed BM chimeras of the type in Fig. 2 were analyzed for CD8αα T cells in IELs and LPLs. The ratios of *Gpr18*$^{-/-}$ versus WT were connected for each mouse. (C) Retrovirus-transduced *Gpr18*$^{-/-}$ BM chimeras of the type in Fig. 3 were analyzed for CD8αα T cells in IELs and LPLs. The ratios of Gpr18-transduced versus untransduced donor-derived cells were connected for each mouse. Data are representative of more than three experiments throughout.

MATERIALS AND METHODS

Mice. C57BL/6J (B6, CD45.2) and congenic B6 CD45.1$^+$ mice were obtained from the Jackson Laboratory, and these strains were intercrossed to generate B6 CD45.1/2 F1 mice. CCR9-deficient mice (Uehara et al., 2002) were obtained from P. Love (National Institutes of Health, Bethesda, MD) and provided by E. Verdin (University of California, San Francisco [UCSF], San Francisco, CA). GPR18-deficient mice were generated by Ozgene Pty Ltd. using the Cre/loxP system. In brief, three DNA fragments (a 4-kb 5′ homology arm, a 1.4-kb floxed arm containing the single *Gpr18* exon, and a 4-kb 3′ homology arm) were generated by nested PCR from C57BL/6 mouse genomic DNA and cloned into the pOzIII vector (Ozgene Pty Ltd.). The targeting vector was linearized and electroporated into B6-derived embryonic stem cells. Positive clones were screened and confirmed with Southern blot. Chimeras were bred to B6 mice, and germline transmission was confirmed by allele-specific PCR. *Gpr18* floxed mice were intercrossed to actin-Cre transgenic mice to obtain *Gpr18* germline deleted mice. To generate BM chimeras, CD45.1$^+$ B6 mice were irradiated by exposure to 1,100 rad of γ-irradiation in two doses 3 h apart and i.v. injected with 2×10^6 total BM cells from CD45.1/2 WT plus 2×10^6 total BM cells from CD45.2 mice of each genotype as indicated (*Gpr18*$^{+/-}$, *Gpr18*$^{-/-}$, or *Ccr9*$^{-/-}$) and analyzed after 2–3 mo. All chimeras appeared healthy at the time of analysis. Although the input cells were mixed at a 1:1 ratio, the reconstitution efficiencies of the different donor BMs were not always identical, a common occurrence in mixed BM chimera studies. Animals were housed in a specific pathogen–free environment in the Laboratory Animal Research Center at the UCSF, and all experiments conformed to ethical principles and guidelines approved by the UCSF Institutional Animal Care and Use Committee.

Cell preparations, adoptive transfer, and migration assays. Thymocyte, splenocyte, and LN cell suspensions were prepared by mashing the organs through 70-µm cell strainers. IELs and LPLs were isolated as described previously (Jiang et al., 2013), with modifications. In brief, Peyer's patches were removed, and then the small intestine was opened longitudinally and washed with PBS containing 0.1% BSA, 100 U/ml penicillin, and 100 µg/ml streptomycin three times. The intestines were then shaken with prewarmed DMEM containing penicillin, streptomycin, and 5% FCS for 30 min at 225 rpm, 37°C. Supernatants were separated on a 30–40–80% Percoll density gradient (GE Healthcare), and the cells that layered between the 40–80% fractions were collected as IELs. After IEL isolation, tissues were shaken in RPMI 1640 containing 5 mM EDTA and 5% FCS at 175 rpm, 37°C for 15 min. This step was repeated four times and the supernatants were discarded. LPLs were then isolated after digestion in RPMI-1640 supplemented with 0.5 mg/ml collagenase type II (Worthington Biochemical Corporation), 0.1 mg/ml DNase I (Sigma-Aldrich), and 10% FCS at 200 rpm, 37°C for 30 min. Released cells were then subjected to Percoll fractionation as described above for isolation of IELs. For IEL adoptive transfer, freshly isolated 3–5 million IELs of each genotype were i.v. co-transferred into recipients. For transfers of T cells activated to induce CCR9 expression, T cells from LNs of each genotype were stimulated with plate-bound CD3 and CD28 plus 100 ng/ml retinoic acid for 3 d and then resuspended in complete RPMI-1640 media with 100 U/ml IL-2 plus 100 ng/ml retinoic acid. At day 5, cells were harvested and transferred into WT recipients. Transwell migration assays were with 5-µm transwells and were performed as described previously (Ngo et al., 1998) using 10^6 IELs prepared by the Percoll density gradient method above. CCL25 and CXCL10 were obtained from BioLegend; CXCL12 was obtained from PeproTech; *N*-arachidonoyl-glycine and 2-arachidonyl-glycerol were obtained from Enzo Life Science and Sigma-Aldrich, respectively.

Antibodies and flow cytometry. Cells were stained using standard procedures for surface markers. The following monoclonal antibodies were used for flow cytometry: TCRγδ (GL3; BD or BioLegend), TCRβ (H57; BioLegend), CD4 (GK1.5; BioLegend), CD8α (53.6.7; Tonbo Bio), CD8β (H35; eBioscience), Thy1.2 (30-H12; BD), Granzyme B (GB11; Invitrogen), CD45.1 (A20; BioLegend), and CD45.2 (104; BioLegend). Vγ7 antibody was provided by P. Pereira (Institut Pasteur, Paris, France). CD8αα cells were gated as $CD8\alpha^+CD8\beta^-$. For cytokine analysis, freshly isolated IELs were stimulated with 40 ng/ml PMA (Sigma-Aldrich) and 4 µg/ml ionomycin (Sigma-Aldrich) for 4.5 h in the presence of GolgiPlug (BD) in complete RPMI-1640 media. Cells were then intracellularly stained for IFN-γ (XMG1.2; BioLegend) and TNF (MP6-XT22; eBioscience) with Cytoperm/Cytofix reagents (BD) according to the manufacturer's instructions. For BrdU incorporation analysis, mice were given water containing 0.5 mg/ml BrdU for 7 d. Staining was performed with a BrdU flow kit (BD) according to the manufacturer's instructions. Annexin V staining of fresh IELs was performed with the Annexin V staining kit (BD).

Immunofluorescence. Cryosections of 7 µm were fixed and stained as previously described (Wang et al., 2011) with the following first antibodies: Laminin (Invitrogen), CD8α (53.6.7; Tonbo Bio), TCRγδ (GL3; BD or BioLegend), and E-cadherin (GG3A; BD). Images were all acquired with AxioVision using an Axio Observer Z1 microscope (Carl Zeiss).

Intravital two-photon microscopy. Mice were i.v. injected with 10 µg anti–CD8α-PE (BioLegend) 5 h before imaging. After anesthetization, mice were injected i.v. with Hoechst 33342 dye (Invitrogen), and the distal duodenum was exposed and opened along the antimesenteric border, as described previously (Edelblum et al., 2012). The mucosal surface was placed against a coverslip bottom of a 3D-printed cassette containing PBS. Images were acquired with ZEN2012 (Carl Zeiss) using a 7MP two-photon microscope (Carl Zeiss) equipped with a Chameleon laser (Coherent). Excitation wavelength was 880 nm. Images were acquired by taking 21-µm Z-stacks at 3-µm steps every 20 s. Each XY plane spans 512 × 512 μm^2. Videos were made and analyzed with Imaris 7.4 ×64 (Bitplane).

Online supplemental material. Videos 1 and 2 show the real-time imaging of $CD8\alpha^+$ IEL migration in $Gpr18^{+/-}$ and $Gpr18^{-/-}$ duodenum, respectively. Online supplemental material is available at http://www.jem.org/cgi/content/full/jem.20140646/DC1.

Thanks to Jinping An for expert help with the mouse colony, Ying Xu for QPCR analysis, Jagan Muppidi for help with epitope tagging, Hsin Chen for imaging help, and Steven Rosen, Tangsheng Yi, Hayakazu Sumida and Michael Barnes for helpful discussions.

X. Wang is an Associate and J.G. Cyster is an Investigator of the Howard Hughes Medical Institute. This work was supported in part by National Institutes of Health grant AI40098.

The authors declare no competing financial interests.

Submitted: 7 April 2014
Accepted: 10 October 2014

REFERENCES

Abadie, V., V. Discepolo, and B. Jabri. 2012. Intraepithelial lymphocytes in celiac disease immunopathology. *Semin. Immunopathol.* 34:551–566. http://dx.doi.org/10.1007/s00281-012-0316-x

Allen, C.D., K.M. Ansel, C. Low, R. Lesley, H. Tamamura, N. Fujii, and J.G. Cyster. 2004. Germinal center dark and light zone organization is mediated by CXCR4 and CXCR5. *Nat. Immunol.* 5:943–952. http://dx.doi.org/10.1038/ni1100

Arnon, T.I., Y. Xu, C. Lo, T. Pham, J. An, S. Coughlin, G.W. Dorn, and J.G. Cyster. 2011. GRK2-dependent S1PR1 desensitization is required for lymphocytes to overcome their attraction to blood. *Science.* 333:1898–1903. http://dx.doi.org/10.1126/science.1208248

Arstila, T., T.P. Arstila, S. Calbo, F. Selz, M. Malassis-Seris, P. Vassalli, P. Kourilsky, and D. Guy-Grand. 2000. Identical T cell clones are located within the mouse gut epithelium and lamina propia and circulate in the thoracic duct lymph. *J. Exp. Med.* 191:823–834. http://dx.doi.org/10.1084/jem.191.5.823

Chennupati, V., T. Worbs, X. Liu, F.H. Malinarich, S. Schmitz, J.D. Haas, B. Malissen, R. Förster, and I. Prinz. 2010. Intra- and intercompartmental movement of γδ T cells: intestinal intraepithelial and peripheral γδ T cells represent exclusive nonoverlapping populations with distinct migration characteristics. *J. Immunol.* 185:5160–5168. http://dx.doi.org/10.4049/jimmunol.1001652

Cheroutre, H., F. Lambolez, and D. Mucida. 2011. The light and dark sides of intestinal intraepithelial lymphocytes. *Nat. Rev. Immunol.* 11:445–456. http://dx.doi.org/10.1038/nri3007

Edelblum, K.L., L. Shen, C.R. Weber, A.M. Marchiando, B.S. Clay, Y. Wang, I. Prinz, B. Malissen, A.I. Sperling, and J.R. Turner. 2012. Dynamic migration of γδ intraepithelial lymphocytes requires occludin. *Proc. Natl. Acad. Sci. USA.* 109:7097–7102. http://dx.doi.org/10.1073/pnas.1112519109

Gray, E.E., K. Suzuki, and J.G. Cyster. 2011. Cutting edge: Identification of a motile IL-17-producing γδ T cell population in the dermis. *J. Immunol.* 186:6091–6095. http://dx.doi.org/10.4049/jimmunol.1100427

Guy-Grand, D., P. Vassalli, G. Eberl, P. Pereira, O. Burlen-Defranoux, F. Lemaitre, J.P. Di Santo, A.A. Freitas, A. Cumano, and A. Bandeira. 2013. Origin, trafficking, and intraepithelial fate of gut-tropic T cells. *J. Exp. Med.* 210:1839–1854. http://dx.doi.org/10.1084/jem.20122588

Hayday, A., E. Theodoridis, E. Ramsburg, and J. Shires. 2001. Intraepithelial lymphocytes: exploring the Third Way in immunology. *Nat. Immunol.* 2:997–1003. http://dx.doi.org/10.1038/ni1101-997

Heilig, J.S., and S. Tonegawa. 1986. Diversity of murine gamma genes and expression in fetal and adult T lymphocytes. *Nature.* 322:836–840. http://dx.doi.org/10.1038/322836a0

Inoue, A., J. Ishiguro, H. Kitamura, N. Arima, M. Okutani, A. Shuto, S. Higashiyama, T. Ohwada, H. Arai, K. Makide, and J. Aoki. 2012. TGFα shedding assay: an accurate and versatile method for detecting GPCR activation. *Nat. Methods.* 9:1021–1029. http://dx.doi.org/10.1038/nmeth.2172

Islam, S.A., and A.D. Luster. 2012. T cell homing to epithelial barriers in allergic disease. *Nat. Med.* 18:705–715. http://dx.doi.org/10.1038/nm.2760

Jiang, W., X. Wang, B. Zeng, L. Liu, A. Tardivel, H. Wei, J. Han, H.R. MacDonald, J. Tschopp, Z. Tian, and R. Zhou. 2013. Recognition of gut microbiota by NOD2 is essential for the homeostasis of intestinal intraepithelial lymphocytes. *J. Exp. Med.* 210:2465–2476. http://dx.doi.org/10.1084/jem.20122490

Johansson-Lindbom, B., and W.W. Agace. 2007. Generation of gut-homing T cells and their localization to the small intestinal mucosa. *Immunol. Rev.* 215:226–242. http://dx.doi.org/10.1111/j.1600-065X.2006.00482.x

Kohno, M., H. Hasegawa, A. Inoue, M. Muraoka, T. Miyazaki, K. Oka, and M. Yasukawa. 2006. Identification of *N*-arachidonylglycine as the endogenous ligand for orphan G-protein-coupled receptor GPR18. *Biochem. Biophys. Res. Commun.* 347:827–832. http://dx.doi.org/10.1016/j.bbrc.2006.06.175

Kunkel, E.J., D.J. Campbell, and E.C. Butcher. 2003. Chemokines in lymphocyte trafficking and intestinal immunity. *Microcirculation.* 10:313–323. http://dx.doi.org/10.1080/mic.10.3-4.313.323

Laky, K., L. Lefrançois, and L. Puddington. 1997. Age-dependent intestinal lymphoproliferative disorder due to stem cell factor receptor deficiency: parameters in small and large intestine. *J. Immunol.* 158:1417–1427.

Lambolez, F., M. Kronenberg, and H. Cheroutre. 2007. Thymic differentiation of TCR$\alpha\beta^+$ CD8$\alpha\alpha^+$ IELs. *Immunol. Rev.* 215:178–188. http://dx.doi.org/10.1111/j.1600-065X.2006.00488.x

Lesley, R., Y. Xu, S.L. Kalled, D.M. Hess, S.R. Schwab, H.B. Shu, and J.G. Cyster. 2004. Reduced competitiveness of autoantigen-engaged B cells due to increased dependence on BAFF. *Immunity.* 20:441–453. http://dx.doi.org/10.1016/S1074-7613(04)00079-2

Li, Y., S. Innocentin, D.R. Withers, N.A. Roberts, A.R. Gallagher, E.F. Grigorieva, C. Wilhelm, and M. Veldhoen. 2011. Exogenous stimuli maintain intraepithelial lymphocytes via aryl hydrocarbon receptor activation. *Cell.* 147:629–640. http://dx.doi.org/10.1016/j.cell.2011.09.025

Lodolce, J.P., D.L. Boone, S. Chai, R.E. Swain, T. Dassopoulos, S. Trettin, and A. Ma. 1998. IL-15 receptor maintains lymphoid homeostasis by supporting lymphocyte homing and proliferation. *Immunity.* 9:669–676. http://dx.doi.org/10.1016/S1074-7613(00)80664-0

Ma, L.J., L.F. Acero, T. Zal, and K.S. Schluns. 2009. Trans-presentation of IL-15 by intestinal epithelial cells drives development of CD8$\alpha\alpha$ IELs. *J. Immunol.* 183:1044–1054. http://dx.doi.org/10.4049/jimmunol.0900420

McHugh, D., J. Wager-Miller, J. Page, and H.B. Bradshaw. 2012. siRNA knockdown of GPR18 receptors in BV-2 microglia attenuates *N*-arachidonoyl glycine-induced cell migration. *J. Mol. Signal.* 7:10. http://dx.doi.org/10.1186/1750-2187-7-10

Ngo, V.N., H.L. Tang, and J.G. Cyster. 1998. Epstein-Barr virus-induced molecule 1 ligand chemokine is expressed by dendritic cells in lymphoid tissues and strongly attracts naive T cells and activated B cells. *J. Exp. Med.* 188:181–191. http://dx.doi.org/10.1084/jem.188.1.181

Pabst, O., L. Ohl, M. Wendland, M.A. Wurbel, E. Kremmer, B. Malissen, and R. Förster. 2004. Chemokine receptor CCR9 contributes to the localization of plasma cells to the small intestine. *J. Exp. Med.* 199:411–416. http://dx.doi.org/10.1084/jem.20030996

Stenstad, H., M. Svensson, H. Cucak, K. Kotarsky, and W.W. Agace. 2007. Differential homing mechanisms regulate regionalized effector CD8$\alpha\beta^+$ T cell accumulation within the small intestine. *Proc. Natl. Acad. Sci. USA.* 104:10122–10127. http://dx.doi.org/10.1073/pnas.0700269104

Sumaria, N., B. Roediger, L.G. Ng, J. Qin, R. Pinto, L.L. Cavanagh, E. Shklovskaya, B. Fazekas de St Groth, J.A. Triccas, and W. Weninger. 2011. Cutaneous immunosurveillance by self-renewing dermal $\gamma\delta$ T cells. *J. Exp. Med.* 208:505–518. http://dx.doi.org/10.1084/jem.20101824

Thien, M., T.G. Phan, S. Gardam, M. Amesbury, A. Basten, F. Mackay, and R. Brink. 2004. Excess BAFF rescues self-reactive B cells from peripheral deletion and allows them to enter forbidden follicular and marginal zone niches. *Immunity.* 20:785–798. http://dx.doi.org/10.1016/j.immuni.2004.05.010

Uehara, S., A. Grinberg, J.M. Farber, and P.E. Love. 2002. A role for CCR9 in T lymphocyte development and migration. *J. Immunol.* 168:2811–2819. http://dx.doi.org/10.4049/jimmunol.168.6.2811

Wang, X., B. Cho, K. Suzuki, Y. Xu, J.A. Green, J. An, and J.G. Cyster. 2011. Follicular dendritic cells help establish follicle identity and promote B cell retention in germinal centers. *J. Exp. Med.* 208:2497–2510. http://dx.doi.org/10.1084/jem.20111449

Wurbel, M.A., M. Malissen, D. Guy-Grand, E. Meffre, M.C. Nussenzweig, M. Richelme, A. Carrier, and B. Malissen. 2001. Mice lacking the CCR9 CC-chemokine receptor show a mild impairment of early T- and B-cell development and a reduction in T-cell receptor $\gamma\delta^+$ gut intraepithelial lymphocytes. *Blood.* 98:2626–2632. http://dx.doi.org/10.1182/blood.V98.9.2626

Wurbel, M.A., M. Malissen, D. Guy-Grand, B. Malissen, and J.J. Campbell. 2007. Impaired accumulation of antigen-specific CD8 lymphocytes in chemokine CCL25-deficient intestinal epithelium and lamina propria. *J. Immunol.* 178:7598–7606. http://dx.doi.org/10.4049/jimmunol.178.12.7598

Yin, H., A. Chu, W. Li, B. Wang, F. Shelton, F. Otero, D.G. Nguyen, J.S. Caldwell, and Y.A. Chen. 2009. Lipid G protein-coupled receptor ligand identification using β-arrestin PathHunter assay. *J. Biol. Chem.* 284:12328–12338. http://dx.doi.org/10.1074/jbc.M806516200